

INFLUENCE OF BISMUTH IMPURITY ON THE SOLIDIFICATION KINETIC AND MICROSTRUCTURE OF Gd-CONTAINING Al-7Si-0.3Mg CAST ALLOYS

¹Ozen GURSOY, ¹Giulio TIMELLI

¹University of Padova, Department of Management and Engineering, Vicenza, Italy, EU,
yozen.gursoy@phd.unipd.it, timelli@gest.unipd.it

<https://doi.org/10.37904/metal.2023.4628>

Abstract

Recycled Al-Si alloys are an important raw material for sustainable and green production due to their low energy consumption. However, various impurity elements, such as Bi, coming from the scraps or recycling process can deteriorate the mechanical properties of the final product. After the limitation of Pb-containing products due to their toxicity by the European Union, Bi content in secondary Al-Si alloys has continuously increased. Bi can interact with other alloying elements affecting the final microstructure and consequently the tensile properties. On the other hand, several investigations about the effect of lanthanide addition into the Al-Si alloys have been performed in recent years. Some lanthanide elements can refine the primary α -Al and modify/refine the eutectic Si crystals. The aim of this work is to study the influence of Bi as a trace element over Gd-containing Al-7Si-0.3Mg alloys. Alloys containing 200 ppm Bi as impurity have been treated by Gd. Two-thermocouple thermal analysis and microstructural investigations were performed to investigate the changes in the solidification sequence and microstructure of the alloys. The results demonstrated that Gd is ineffective on the refinement of α -Al dendrites while it decreases the growth temperature of eutectic reaction and refines the eutectic Si crystals of the Al-7Si-0.3Mg alloy. Unlike traditional eutectic Si modifiers, such as Na and Sr, the efficiency of Gd addition on the eutectic was not influenced by Bi impurity. No Bi/Gd interaction was detected. Additionally, SEM investigations showed that Bi-rich phases are located in the growth front of the GdAl_2Si_2 phases.

Keywords: Bismuth, gadolinium, interaction, solidification, microstructure

1. INTRODUCTION

Al-Si alloys are typically considered primary foundry alloys, which are produced using bauxite ore as the main raw material. However, it is also possible to produce these alloys using aluminum scrap and recycling, which is known as the secondary route for aluminum production. Compared to the primary route, the secondary method can reduce energy consumption and greenhouse gas emissions by around 95 % [1]. By using this approach, it is estimated that producing one ton of secondary Al alloy can save up to 14,000 kWh of energy and result in about 350 kg of CO₂ emissions [1]. Overall, secondary Al-Si alloys provide a favorable balance between mechanical properties and material costs.

Although secondary Al-Si alloys are generally less expensive than primary alloys, the presence of impurities from scrap or recycling processes can compromise their mechanical properties. One impurity that can affect these alloys is Bi, which is often present in free-cutting wrought aluminum alloys that are substituting lead-containing alloys [2]. Due to concerns about the toxicity of lead and its products, restrictions on the use of Pb-containing materials have been in place in the European Union since 2008 [3]. Consequently, the use of Bi-containing alloys has increased, leading to a rise in Bi contamination in secondary Al-Si alloys.

It has been extensively studied that the machinability of Al alloys can be improved through the addition of bismuth [4–6]. To enhance the tensile and wear resistance properties of hypoeutectic and hypereutectic Al-Si

alloys, bismuth is used as a chemical refiner for the eutectic silicon flakes [7]. On the other hand, Bi, even in trace amounts, can counteract the effects of other alloying additions or preliminary molten metal treatments, thereby deteriorating the final microstructure and tensile performance of the alloy. Researchers have shown that the presence of bismuth in chemically modified Al-Si foundry alloys can increase the eutectic growth temperature, leading to a transition from a fibrous to a plate-like eutectic Si structure [3,8,9]. As a result, there is a reduction in the available modifier element for eutectic Si modification.

Recent works have focused on the impact of lanthanide elements on the microstructure of Al-Si alloys. Studies have demonstrated that some lanthanides can refine the primary α -Al grains and modify the eutectic Si crystals in the alloys [10]. Additionally, it has been shown that lanthanide elements can be an effective eutectic modifier, leading to restricted nucleation and growth of eutectic Si crystals [11]. Among those elements, gadolinium (Gd) has recently gained attention as an addition element to Al-Si casting alloys. It has been observed that Gd addition can decrease grain size due to induced constitutional undercooling [12,13]. Furthermore, it is suggested that the heavy enrichment of Gd atoms in front of eutectic cells may interfere with the growth orientation of Si phases.

In this study, the impact of Bi as an impurity element on Gd-containing Al-7Si-0.3Mg alloy was investigated. The focus is on understanding potential Bi/Gd interactions, changes in the solidification sequence, and their effects on the final microstructure of the alloy. This research is particularly relevant, as recycled Al alloys may contain higher levels of Bi as an impurity. Therefore, gaining a better understanding of Bi/Gd interactions during the preliminary molten metal treatments is crucial for grain refinement and eutectic modification of Al-Si-based alloys.

2. EXPERIMENTAL PROCEDURE

In the present work, a commercial purity Al-7Si-0.3Mg alloy was used as the base alloy. The chemical composition of the base alloy was measured by optical emission spectrometry (OES) and it is listed in **Table 1**. The melt was prepared by introducing around 2 kg of ingot pieces into a SiC crucible, which was then heated to 750 ± 5 °C using an electrical furnace. The molten bath was subsequently kept in the furnace for 30 minutes to promote uniformity. Weighted AlBi9 and AlGd5 master alloys in the form of waffle ingots were added to achieve the desired Bi and Gd levels. The Bi and Gd levels in the different experimental alloys are listed in **Table 1**. After the addition of Bi and/or Gd into the molten bath, the contact time between the Bi/Gd additives and the melt was applied as 45 minutes, according to the previously reported study [14]. After the molten bath was skimmed and gently stirred, it was carefully poured into a BN-coated steel cup measuring 45 mm in diameter and 60 mm in height, which had been preheated to 550 ± 5 °C, providing a cooling rate of approximately 0.2 °C/s.

Table 1 Chemical composition of the experimental alloys (wt%).

Alloy	Si	Fe	Cu	Mg	Ti	Bi	Gd	Al
Base	6.98	0.0591	0.0017	0.313	0.119	-	-	Bal.
Base + Bi	7.17	0.0564	0.0031	0.291	0.128	0.0240	-	Bal.
Base + Gd	7.12	0.0591	0.0011	0.310	0.108	-	0.458	Bal.
Base + Bi + Gd	7.01	0.0892	0.0031	0.306	0.120	0.0236	0.465	Bal.

The solidification path and characteristic temperatures of experimental alloys were monitored using a computer-aided two-thermocouple thermal analysis technique. After pouring the melt into a pre-heated steel cup, a K-type thermocouple ($\varnothing 1$ mm) was inserted into the melt through a ceramic lid, covered by a tight stainless-steel tube, and located along the central axis. The tip of the thermocouple was positioned 30 mm above the bottom of the sample. The procedure of thermal analyses was previously reported in detail

elsewhere [3]. To determine the characteristic temperatures of the α -Al phase and Al-Si eutectic reaction, cooling curves and their corresponding derivative curves (dT/dt) were plotted for each alloy. Phase reactions were identified by analyzing the change in slope of the cooling curve, which corresponded to the first derivative of the cooling curve [15].

The macro- and microstructural evolutions of the experimental alloys were investigated, and their results were correlated with those obtained from thermal analyses. Samples for thermal analyses were extracted from close to the thermocouple's tip. Samples were then mounted, grounded, and polished using standard metallography techniques. To reveal the grain boundaries, the polished samples were etched in a solution of 30 vol.% CuCl_2 and 70 vol.% H_2O and then immersed in a solution of 86 vol.% HNO_3 and 14 vol.% HF to improve contrast [16]. The grain size was measured using the intercept method, as specified in the ASTM standard E112-12 [17]. To determine the secondary dendrite arm spacing (SDAS) of the polished samples, a microstructural investigation was performed using an optical microscope and image analysis software. At least 50 measurements were taken for each sample to obtain an accurate average SDAS value. Furthermore, the microstructural investigation focused on studying the size and morphology of eutectic Si particles, which were analyzed as functions of the level of Bi impurity and the Gd content. The equivalent circular diameter and aspect ratio of eutectic Si crystals were measured. Secondary intermetallic phases, such as Mg_2Si and Fe-bearing, were excluded from the measurements. A statistical average was obtained by analyzing over 1000 particles from each sample. To identify the intermetallic phases, a field emission gun scanning electron microscope (FEG-SEM) that was equipped with an energy-dispersive spectrometer (EDS) unit were used.

3. RESULTS AND DISCUSSION

3.1 Thermal Analysis

Figure 1 shows the cooling curves and their first derivatives of the experimental alloys containing different Bi and Gd amounts. The precipitation regions of α -Al and Al-Si eutectic can be easily observed [18]. The characteristic temperatures of the experimental alloys are listed in the **Table 2**. The nucleation of α -Al in the base alloy took place at 619.2 °C while the growth temperature ($T_{G,\alpha}$) was measured at 618.9 °C, showing a recalescence undercooling ($\Delta T_{R,\alpha}$) of 2.6 °C. Bi as impurity and Gd, neither individually nor combined, in the alloy did not alter the solidification path and the characteristic temperatures of the primary α -Al phase (see **Figure 1** and **Table 2**).

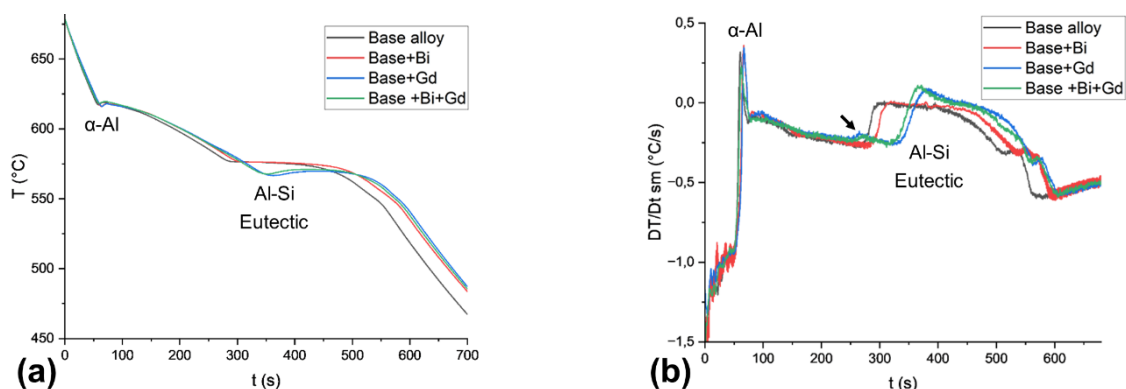


Figure 1 Cooling curves (a) and their corresponding derivatives (b) referred to the experimental alloys

The formation of Al-Si eutectic in the base alloy began at 578.9 °C and its $T_{G,eu}$ was at 575.5 °C. No undercooling was observed during the precipitation of eutectic in the base alloy. The phenomenon of eutectic nucleation in Al-Si alloys was investigated by McDonald et al. [19]. It was found that commercial alloys exhibited a high degree of eutectic nucleation, mainly because of the presence of common nuclei such as AlP

compounds. Commercial Al-Si alloys frequently contain impurities of phosphorus, and concentrations exceeding 3 ppm were found to promote the formation of pre-eutectic AIP particles. These particles act as heterogeneous nucleation sites during the solidification process of the alloy, facilitating the nucleation of eutectic Si.

Table 2 Characteristic temperatures (in °C) from thermal analysis of the experimental alloys.

Alloy	$T_{N,\alpha}$	$T_{min,\alpha}$	$T_{G,\alpha}$	$\Delta T_{R,\alpha}$	$T_{N,eu}$	$T_{min,eu}$	$T_{G,eu}$	$\Delta T_{R,eu}$
Base	619.2	616.3	618.9	2.6	578.9	575.5	575.5	0
Base + Bi	618.7	616.1	618.2	2.1	578.9	575.3	575.3	0
Base + Gd	618.7	616.1	618.0	1.9	569.9	566.6	569.7	3.1
Base + Bi + Gd	619.6	616.4	618.0	1.6	569.3	566.2	569.6	3.4

While Bi impurity in the alloy did not affect the eutectic reaction and the characteristic temperatures of eutectic in the alloy containing Bi impurity remained nearly the same, the eutectic plateau was significantly depressed by the addition of Gd. In detail, the eutectic of Gd containing alloy nucleated at 569.9 °C, $T_{G,eu}$ was measured at 569.7 °C, and the reaction showed some degree of undercooling. It is also possible to observe the increased peak of eutectic reaction in the derivative curve of Gd containing alloy. On the other hand, a pre-eutectic peak indicated in **Figure 1b** by an arrow was detected at around 591 °C in the derivative curve of Gd containing alloy related to the precipitation of Gd-rich phases.

When the Gd was added into the alloy containing Bi impurity, it was observed that cooling curve of the eutectic and corresponding derivative of the alloy showed the same path with Gd containing Bi-free alloy. The characteristic temperatures of Gd containing alloy with Bi impurity remained almost the same with the ones from Gd containing Bi-free alloy. It can be stated that eutectic plateau depressed by Gd is not influenced by Bi impurity. Furthermore, no additional peak was detected related to Bi-bearing phases.

3.2 Macro- and Microstructural Investigations

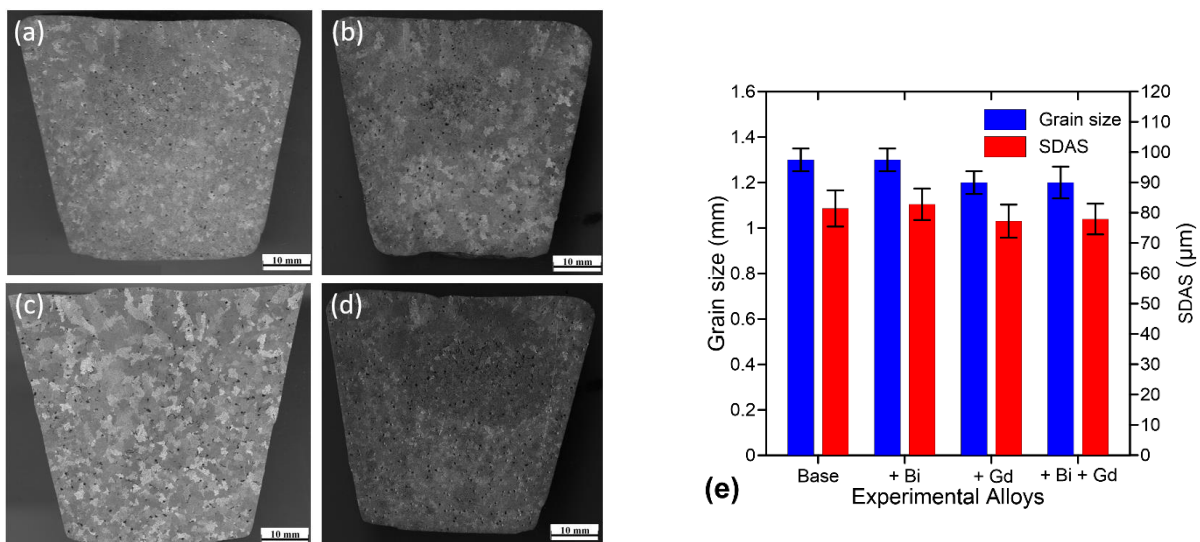


Figure 2 Macrographs of Gd-free (base) (a), Bi-containing (base + Bi) (b), Gd-containing (c), Bi- and Gd-containing (base + Bi + Gd) alloys and corresponding average grain size and SDAS values (e) of the experimental alloys.

Figure 2 shows the macrographs of the experimental alloys with Bi and/or Gd contents. About 240 ppm Bi impurity or 0.5 wt% of Gd content or both at the same time did not alter the grain structure of the α -Al. It can

be observed from **Figure 2e** that although average grain size and SDAS values are nearly the same in the experimental alloys, they are slightly lower in Gd-containing alloys due to the growth restriction effect of Gd. It is previously reported that Bi impurity in such low level (~240 ppm) has no influence on α -Al grains [8,20]. It has been stated nucleant particles in the form of XAl_3 provide heterogeneous nucleation on the primary α -Al grains [21,22]. In this study, $GdAl_3$ particles were not identified in Gd-containing alloys. Only the hexagonal $GdAl_2Si_2$ intermetallics, which precipitate after the formation of primary α -Al grains, were detected in the microstructure.

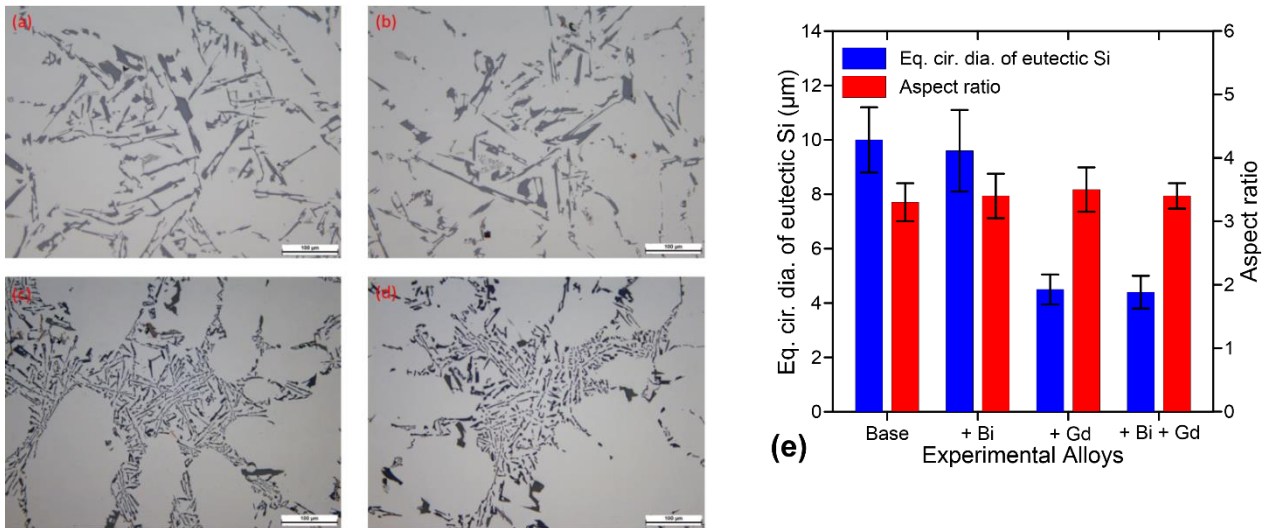


Figure 3 Eutectic microstructures of Gd-free (base) (a), Bi-containing (base + Bi) (b), Gd-containing (c), Bi- and Gd-containing (base + Bi + Gd) alloys and corresponding average equivalent circular diameter and aspect ratio values (e) of the eutectic Si crystals in the experimental alloys.

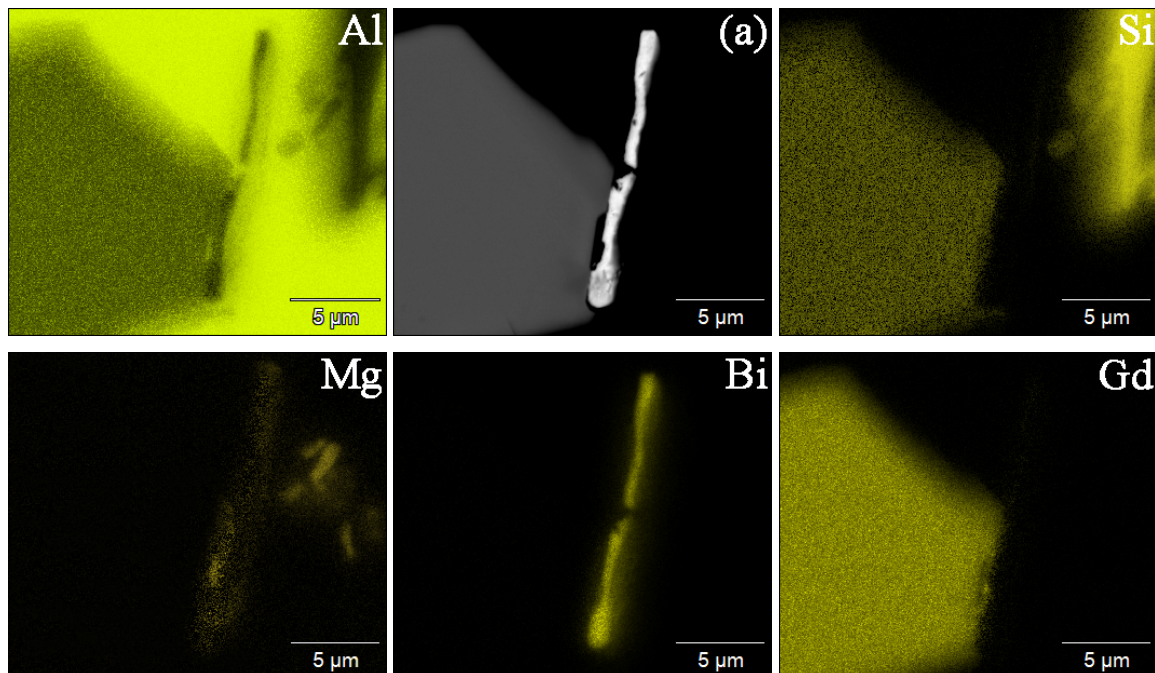


Figure 4 Backscattered electron FEG-SEM image of Gd-rich intermetallic and Bi-bearing compound (a) in Bi- and Gd containing alloy (Base + Bi + Gd) and corresponding energy-dispersive spectrometer (EDS) composition maps, showing the distribution of Al, Si, Mg, Bi, and Gd.

Figure 3 shows the eutectic microstructures of the experimental alloys and corresponding average equivalent circular diameter and aspect ratio of eutectic Si crystals. It can be seen that eutectic Si crystals were coarse and flak-like in the base alloy. In both Gd-containing alloys (Base + Gd and Base + Bi + Gd), eutectic Si particles were refined with the addition of Gd. **Figure 3e** shows that average equivalent circular diameter of eutectic Si decreased in both Gd-containing alloys. Since the flake-to-fibrous transition doesn't take place during the refinement of the eutectic Si crystals, average aspect ratio of the experimental alloys remained nearly the same. Bi impurity didn't affect the eutectic structure neither in Gd-free alloy nor in Gd-containing alloy (**Figures 3b, d and e**). It is clear how cooling path, cooling rate and characteristic temperatures are strongly correlated with the microstructure changes. Modification/refinement of eutectic structure in Al-Si alloys can be provided through the chemically poisoning of AIP, that is the main nucleant of eutectic Si crystals, so that Si crystals can no longer nucleate on AIP. Moreover, diffusion of the chemical modifier/refiner element to the solid/liquid interface restricts the growth of the Si crystals, it therefore decreases the size of the Si crystals.

A backscattered electron FEG-SEM image of bright Bi-bearing and gray Gd-rich intermetallic particles in Bi- and Gd-containing alloy and the corresponding EDS composition maps are shown in **Figure 4**. Al, Si and Gd were evident in gray polyhedral particle, while only Bi and Mg elements were detected on the bright elongated particle. It is recently reported that Mg_3Bi_2 compounds precipitate in Mg-enriched Bi-rich melt droplets at a higher temperature than the temperature of Al-Si eutectic reaction and it is a stable intermetallic due to a higher melting temperature [3]. In the current study, it was found that the precipitation of $GdAl_2Si_2$ intermetallic took place at around 591 °C as a pre-eutectic reaction. Mg_3Bi_2 was pushed towards the melt during the growth of $GdAl_2Si_2$ particles and diffusion of their elements were not observed between these two compounds. Therefore, it can be stated that no poisoning of Gd occurred.

4. CONCLUSION

The effect of Bi impurity on the solidification path and microstructure of Gd-free and Gd-containing Al-7Si-0.3Mg alloys have been investigated. The key conclusions are as follows:

- Gd is ineffective on grain refinement. It slightly decreases the grain size and SDAS due to the growth restriction effect.
- Gd refines the eutectic Si crystals.
- Bi does not counteract with Gd and not effect the macro- and microstructural changes.

ACKNOWLEDGEMENTS

The work was developed with the financial support of Fondazione Cassa di Risparmio di Padova e Rovigo (CariPaRo).

REFERENCES

- [1] BLOMBERG, J., SÖDERHOLM, P. The economics of secondary aluminium supply: An econometric analysis based on European data. *Resources, Conservation and Recycling*. 2009, vol. 53, no. 8, pp. 455-463.
- [2] BSI Standards Publication Aluminium and Aluminium Alloys — Wrought Products — Temper Designations. 2017.
- [3] GURSOY, O., TIMELLI, G. The Role of Bismuth as Trace Element on the Solidification Path and Microstructure of Na-Modified AlSi7Mg Alloys. *Advanced Engineering Materials*. 2023, 2201377.
- [4] BARZANI, M. M., FARAHANY, S., YUSOF, N. M., OURDJINI, A. The influence of bismuth, antimony, and strontium on microstructure, thermal, and machinability of aluminum-silicon alloy. *Materials and manufacturing processes*. 2013, vol. 28, no. 11, pp. 1184-1190.
- [5] BARZANI, M. M., AHMED, S., FARAHANY, S., RAMESH, S., MAHER, I. Investigating the Machinability of Al-Si-Cu cast alloy containing bismuth and antimony using coated carbide insert. *Measurement*. 2015, vol. 62, pp. 170-178.

- [6] TIMELLI, G., BONOLLO, F. Influence of tin and bismuth on machinability of lead free 6000 series aluminium alloys. *Materials Science and Technology*. 2011, vol. 27, no. 1, pp. 291-299.
- [7] COSTA, T. A., MARCELINO D., CASSIO S., EMMANUELLE F., ADRINA P. S., NOÉ Ch., AMAURI G.. Measurement and interrelation of length scale of dendritic microstructures, tensile properties, and machinability of Al-9 wt% Si-(1 wt% Bi) alloys. *The International Journal of Advanced Manufacturing Technology*. 2019, vol. 105, pp. 1391-1410.
- [8] FARAHANY, S., OURDJINI, A., IDRIS, M. H., THAI, L.T. Poisoning effect of bismuth on modification behaviour of strontium in LM25 alloy. *Bulletin of Materials Science*. 2011, vol. 34, pp. 1223-1231.
- [9] FARAHANY, S., DAHLE, A.K., OURDJINI, A., ALIREZA, H.A. Flake-fibrous transition of silicon in near-eutectic Al-11.7 Si-1.8 Cu-0.8 Zn-0.6 Fe-0.3 Mg alloy treated with combined effect of bismuth and strontium. *Journal of Alloys and Compounds*. 2016, vol. 656, pp. 944-956.
- [10] PANDEE, P., PATAKHAM, U., LIMMANEEVICHITR, C. Microstructural evolution and mechanical properties of Al-7Si-0.3 Mg alloys with erbium additions. *Journal of Alloys and Compounds*. 2017, vol. 728, pp. 844-853.
- [11] NOGITA, K., MCDONALD, S.D., DAHLE, A.K. Eutectic modification of Al-Si alloys with rare earth metals. *Materials Transactions*. 2004, vol. 45, no. 2, pp. 323-326.
- [12] LIU, W., WENLONG, X., CONG, X., MAOWEN, L., CHAOLI, M. Synergistic effects of Gd and Zr on grain refinement and eutectic Si modification of Al-Si cast alloy. *Materials Science and Engineering*. 2017 vol. A 693, pp. 93-100.
- [13] SHI, Z., WANG, Q., SHI, Y. ZHAO, G., ZHANG, R. Microstructure and mechanical properties of Gd-modified A356 aluminum alloys. *Journal of Rare Earths*. 2015, vol. 33, no. 9, pp. 1004-1009.
- [14] GURSOY, O., TIMELLI, G. The Effect of the Holding Time on the Microstructure of Gd-Containing AlSi7Mg Alloys. *In Light Metals*. 2022, pp. 779-784. Cham: Springer International Publishing.
- [15] DJURDJEVIC, M.B., IBAN V., GERHARD H. Review of thermal analysis applications in aluminium casting plants. *Revista de Metalurgia*. 2014, vol. 50, no. 1, pp. 1-12.
- [16] VANDER, V., BALDWIN, W. Metallography and Microstructures Handbook. *ASM International: Materials Park*, 2004, OH, USA.
- [17] ASTM E112–12: standard test methods for determining average grain size. *ASTM Int E112–12: 1–27*.
- [18] BACKERUD, L., CHAI, G., TAMMINEN, J. Solidification characteristics of aluminum alloys: Foundry alloys. Vol. 2. *American Foundrymen's Society, Inc.*, 1990, p. 266.
- [19] MCDONALD, S.D., KAZUHIRO, N., DAHLE, A.K. Eutectic nucleation in Al–Si alloys. *Acta materialia*. 2004, vol. 52, no. 14, pp. 4273-4280.
- [20] FARAHANY, S., OURDJINI, A., BAKAR, T.A.A. Bakar, IDRIS, M.H. Role of bismuth on solidification, microstructure and mechanical properties of a near eutectic Al-Si alloys. *Metals and Materials International*. 2014, vol. 20, pp. 929-938.
- [21] WANG, Q., ZHIMING, S., HONG, L., YAMING, L., NINGYU, L., GONG, T., ZHANG, R., LIU, H. Effects of holmium additions on microstructure and properties of A356 aluminum alloys. *Metals*. 2018, vol. 8, no. 10, p. 849.
- [22] HU, X., FUGANG, J., FANRONG, A., HONG, Y. Effects of rare earth Er additions on microstructure development and mechanical properties of die-cast ADC12 aluminum alloy. *Journal of Alloys and Compounds*. 2012, vol. 538, pp. 21-27.